Journal of Computers Vol. 36 No. 2, April 2025, pp. 15-29
https://doi.org/10.63367/19911599202504360200 2

Communication Performance Analysis and Research of UAV Cooperative Non-Orthogonal Multiple Access System

Ying Lin*, Kai-Qin Qin, Xing-Bo Gong, Yong-Wei Xiong, Chan-Fei Wang, and Jian-Bin Xue

School of Computer and Communication, Lanzhou University of Technology, Lanzhou 730050, Gansu, China
bhfrlin@163.com, 2310491385@qq.com, 1986929243@qq.com, 753480104@qq.com,
wangchanfei@163.com, volvoxuejb@126.com

Received 27 February 2024; Revised 21 March 2024; Accepted 21 March 2024

Abstract. In the case of poor communication such as major disasters and forest fire, the use of unmanned aerial vehicle (UAV) as emergency communication relays can realize the normal transmission of signals. In this paper, the performance of cooperative non-orthogonal multiple access (NOMA) communication system based on UAV is studied. First of all, the average achievable rate of the UAV cooperative NOMA communication system under the independent Rayleigh fading channel is analyzed. Mathematical methods are employed to derive expressions for the average achievable rate, outage probability, and throughput. The accuracy of the theoretical results is verified through Monte Carlo simulations. Secondly, the impact of UAV flight altitude on system performance is further analyzed. The results indicate that the communication performance of UAV cooperative NOMA scheme exhibits significant improvement compared to the traditional cooperative communication system.

Keywords: cooperative relay, UAV, non-orthogonal multiple access technology, communication performance

1 Introduction

In recent years, the frequent occurrence of natural disasters in China has hindered the rapid development of China's economy and brought about serious social impacts, especially after the occurrence of natural disasters, the normal work of communication and electricity has been seriously affected, which has brought about great difficulties in post-disaster relief. Unmanned aerial vehicle (UAV) has attracted a lot of attention in the field of wireless communication due to its cost-effective and flexible mobility [1-2]. When confronted with major natural disasters and unexpected occurrence, terrestrial base stations cannot be used normally. UAV in the air can be utilized to allow itself to act as temporary base station or relay due to its random movement and rapid deployment. It enables users on the ground to connect to the network for messaging. Currently, UAV-assisted communication applications include UAV coverage, assisted relay, assisted data acquisition and information dissemination [3]. UAV is indispensable for emergency rescue in response to urgent and sudden disasters. During the China Eastern Airlines crash, technologists used UAV to map and photograph the crash site. UAV aerial base station, together with emergency response vehicles on the ground, can provide communications services in the field.

At present, many scholars at home and abroad have made a great deal of contributory works and researches in optimizing and improving the communication performance of UAV. The height and horizontal position of the UAV can be optimized individually or jointly to meet different Quality of Service (QoS) requirements. In [4], the authors investigated a UAV-assisted data cellular phone system under two commonly used UAV circular flight trajectories and straight-line flight trajectories, they derived an expression of the energy consumption between the UAV and the ground terminal, obtained the optimal launch power and UAV trajectory, and found a trade-off between energy consumption and transmission throughput for UAV work. In [5], the authors investigated the energy efficiency of UAVs for a given trajectory, the models are derived for two communication scenarios dominated by line-of-sight wireless transmission and non-line-of-sight wireless transmission. In [6], the authors proposed an energy saving scheme so as to minimize the UAV flight communication energy and optimize the UAV flight trajectory. In [7], the authors addressed the enhancement of coverage scenarios in a multi-UAV cooperative ground-based cellular heterogeneous network. The article mentions that the joint optimization of UAV position,

* Corresponding Author

beamforming and correlation between the UAV and the ground user is transformed into a mixed integer nonlinear programming problem to obtain the maximum user transmission rate. On the other hand, cooperative communication can effectively increase the transmission rate of user, and enhance the capacity of the communication system. In [8], authors investigated the performance of cooperative non-orthogonal multiple access (NOMA) system combined with power transmission under Rayleigh fading conditions, when there is no direct link between the base station and the remote user. In [9], the authors studied the relay selection problem in cooperative NOMA networks, proposed a novel relay selection scheme, derived an expression for the outage probability, and proved that the proposed relay selection scheme communication system performs better. In [10], the authors investigated cooperative secure beamforming for synchronized wireless information and power transmission in amplify and forward (AF) relay networks. In [11], the authors have analyzed the end-to-end performance of decode-and-forward (DF) cooperative single antenna relaying for communication systems with maximal ratio combining (MRC), derived and validated the expressions of the proposed theory.

As the development of cooperative communication technology becomes more and more mature, traditional communication can no longer satisfy the communication scenarios in mountainous areas or in the case of a major disaster area. Researchers are beginning to gradually focus on techniques that combine NOMA with cooperative UAV communications. In [12], the authors utilized a fixed-wing UAV to serve two terrestrial users by means of downlink NOMA transmission, derived the outage probability for the two terrestrial users, and selected efficient transmission mode to ensure optimal terminals, to achieve user fairness. In [13], the authors modeled the positions of UAV and ground users in a NOMA transmission UAV system, conducted an evaluation of the communication system's performance. In [14], the authors investigated the security, reliability and energy coverage performance of the UAV network communications under both NOMA and orthogonal multiple access (OMA) schemes. In [15], the authors investigated the performance of a system combining a fixed-altitude UAV with NOMA, and derived expressions for the outage probability for the far-end NOMA users and near-end NOMA users. In [16], the authors studied multiple randomly deployed user scenarios, improved the performance of UAV cooperative NOMA systems through joint optimization of layout and power allocation. It is obvious that the above literatures don't analyze the capacity performance of UAV relay cooperative NOMA communication system.

This paper investigated the capacity performance of UAV cooperative NOMA communication system. The contributions of this paper are as follows:

- We mathematically derive the average reachable rate of the system and further derive expressions for the outage probability and throughput.
- We analyze the impact of reachability rate, outage probability, and throughput on the performance of the UAV relay cooperative NOMA, and study the effect of UAV flight altitude on system performance.
- We verify the accuracy of the theoretical derivation using Monte-Carlo simulations.

The paper organized in rest part as the system model is described in Section II. Analysis of System Performance is presented in Section III. Section IV articulates the numerical results and conclusion is presented in Section V.

2 System Model

In the traditional cooperative NOMA system model, the relay operates on the ground. However, in the UAV cooperative NOMA communication system, UAV serve as airborne relays to transmit signals for ground users.

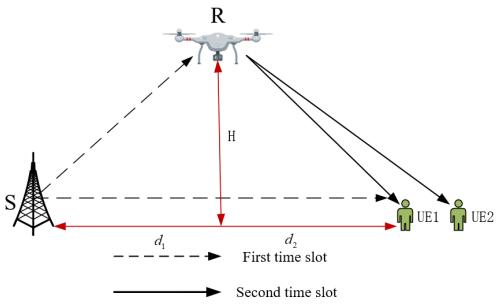

Fig. 1. System model

In this article, it is assumed that all communication links are available throughout the system. The system relies on UAV relays to facilitate normal signal transmission. As illustrated in Fig. 1, similar to the traditional cooperative NOMA system, this system is composed of a source (S), a relay (R), and a destination (D). Assuming the entire communication system is analyzed under independent Rayleigh fading channel conditions, the channel coefficients for Source to UAV (S-R), Source to Destination (S-D), and UAV to Destination (R-D) are denoted by h_{SR}, h_{SD}, h_{RD}. The communication links for the first time slot (TS) are S to R, S to D, and the communication link for the second TS is R to D.

Considering the existence of channel estimation error in practical systems, it is difficult to obtain perfect channel state information, and the channel estimation errors are mainly caused by feedback delay errors. In this system, assuming the estimated channel coefficients is $\hat{h}_i$, the communication channel coefficients can be modeled as $h_i = \hat{h}_i + \kappa e_i$, ($i$ = *SR*, *SD*, *RD*), where $e_i \sim CN(0, \sigma_{e_i}^2)$ denotes the communication channel error vector that can be approximated as a Gaussian random variable, and κ denotes the impact factor of the estimation error. The channel gain for each link can be defined as $g_{SR} = \left|\hat{h}_{SR}\right|^2 / D_1$, $g_{RD} = \left|\hat{h}_{RD}\right|^2 / D_2$, $g_{SD} = \left|\hat{h}_{SD}\right|^2 / D_3$, where $D_1 = \left(\sqrt{\mathrm{H}^2 + d_1^2}\right)^{\alpha_T}$, $D_2 = \left(\sqrt{\mathrm{H}^2 + d_2^2}\right)^{\alpha_T}$, $D_3 = c^{\alpha_T}$, $d_1 + d_2 = c$. H denotes the height of the UAV above the ground, and d_1, d_2 denote the horizontal distances from S to Rand from R to D, respectively. c denotes the distance between S and D. and $\left|\hat{h}_{SR}\right|^2$, $\left|h_{RD}\right|^2$, $\left|h_{SD}\right|^2$ represents exponential distributions with a mean of β_{SR}, β_{RD}, β_{SD}. α_T denotes the link loss factor.

In UAV cooperative NOMA communication, there exists a direct link between S and D. In the first TS, the source transmits two symbols x_1 and x_2 simultaneously to the relay and the destination, it is assumed that a_1 and a_2 are the power allocation coefficient for the source transmission power, and $a_1 + a_2 = 1$, $a_1 > a_2$. According to the NOMA principle, more power is allocated to the weak user, and less power is allocated to the strong user, which ensures higher data rate for the weak user. The signal expressions received by the UAV and the destination are given as:

$$y_{SR} = \left(\hat{h}_{SR} + \kappa e_{SR}\right)\left(\sqrt{a_1 P_S}\, x_1 + \sqrt{a_2 P_S}\, x_2\right) + n_{SR} \tag{1}$$

$$y_{SD} = \left(\hat{h}_{SD} + \kappa e_{SD}\right)\left(\sqrt{a_1 P_S}\, x_1 + \sqrt{a_2 P_S}\, x_2\right) + n_{SD} \tag{2}$$

Where n_{SR} and n_{SD} denote additive white Gaussian noise (AWGN) with zero mean and variance σ^2. P_S denotes the transmit power of the source. e_{SR} denote the S-R channel estimation error. e_{SD} denote the S-D channel estimation error.

In the first TS, the relay decodes the signal of UE1 by treating the signal of UE2 as noise, and cancels UE1 using successive interference cancellation (SIC) to acquire after decoding UE2 signal form (1), Consequently, the signal-to-interference-plus-noise ratio (SINR) for the two users at the UAV relay can be expressed as:

$$\gamma_R^1 = \frac{g_{SR} a_1 P_S}{g_{SR} a_2 P_S + \kappa \sigma_{e_{SR}}^2 P_S + \sigma^2} \tag{3}$$

$$\gamma_R^2 = \frac{g_{SR} a_2 P_R}{\kappa \sigma_{e_{SR}}^2 P_S + \sigma^2} \tag{4}$$

In the second TS, the relay receives the superimposed signal from the source and uses SIC to decode the two signals. Then, the relay re-encodes the two signals and transmits them to the destination. Assuming b_1 and b_2 are the power allocation coefficient of signal in relay, and $b_1 + b_2 = 1$, $b_1 > b_2$. The signal received at the destination from the relay is given as:

$$y_{RD} = \left(\hat{h}_{RD} + \kappa e_{RD}\right)\left(\sqrt{b_1 P_R}\, x_1 + \sqrt{b_2 P_R}\, x_2\right) + n_{RD} \tag{5}$$

Where n_{RD} denote AWGN with zero mean and variance σ^2. P_R denotes the transmit power of the relay. e_{RD} denote the R-D channel estimation error.

The destination does not decode the superimposed signal from the source immediately. Instead, it waits until receiving the signal sent by the relay in the second TS. The destination then employs a joint decoding approach using MRC and SIC to decode the signals from the source and the relay. The received SINR for the destination UE1 and UE2 are given as:

$$\gamma_D^1 = \frac{g_{SD} a_1 P_S}{g_{SD} a_2 P_S + \kappa \sigma_{e_{SD}}^2 P_S + \sigma^2} + \frac{g_{RD} b_1 P_R}{g_{RD} b_2 P_R + \kappa \sigma_{e_{RD}}^2 P_R + \sigma^2} \tag{6}$$

$$\gamma_D^2 = \frac{g_{SD} a_2 P_S}{\kappa \sigma_{e_{SD}}^2 P_S + \sigma^2} + \frac{g_{RD} b_2 P_R}{\kappa \sigma_{e_{RD}}^2 P_R + \sigma^2} \tag{7}$$

Based on the fact that the end-to-end rate of DF relaying is dominated by the weakest link [17], the achievable rate for each user can be expressed as:

$$C_{x_1} = \frac{1}{2} \log_2 (1 + SINR_1) \tag{8}$$

$$C_{x_2} = \frac{1}{2} \log_2 (1 + SINR_2) \tag{9}$$

Where $SINR_1 = \min(\gamma_R^1, \gamma_D^1)$, $SINR_2 = \min(\gamma_R^2, \gamma_D^2)$.

3 Analysis of System Performance

The key performance indicators for wireless communication include average achievable rate, outage probability, and throughput. The following the performance of the system's achievable rate was investigated.

In order to analyze the average achievable rate of the system, it is necessary to know the cumulative distribution function (CDF) of the system. Therefore, the following derivation is performed for the CDF of the SINR for two users.

Theorem 1: The CDF of the SINR for UE1 is given as:

$$F_{SINR_1}(x) = 1 - e^{-\left(\frac{\chi_{SR}\psi(x)}{\beta_{SR}} + \frac{\chi_{SD}\psi(\tau)}{\beta_{SD}}\right)}, \quad 0 < x < a_1 / a_2 \tag{10}$$

Where $\chi_{i,j} = \kappa \sigma_{e_i}^2 \rho_j + 1$, $\rho_j = P_j / \sigma^2$, $i \in \{SR, RD, SD\}$, $j \in \{s, r\}$, $\psi(x) = \frac{xD_1}{(a_1 - a_2 x)\rho_s}$, $\psi(x) = \frac{\tau D_3}{(a_1 - a_2 \tau)\rho_s}$, $\tau = x - b_1 / b_2$.

$$F_{SINR_1}(x) = \Pr(SINR_1 < x) = 1 - \Pr(SINR_1 > x) \tag{11}$$

Proof: The CDF of the SINR for UE1 is proved as follows.

The complementary cumulative distribution function (CCDF) of the SINR for UE1 is as follows:

$$\begin{aligned}\overline{F}_{SINR_1}(x) &= \Pr(SINR_1 > x)\\ &= \Pr\left(\min(\gamma_R^1, \gamma_D^1) > x\right)\\ &= \Pr\left\{\frac{g_{SR}a_1\rho_s}{g_{SR}a_2\rho_s + \kappa\sigma_{e_{SR}}^2\rho_s + 1} > x, \frac{g_{SD}a_1\rho_s}{g_{SD}a_2\rho_s + \kappa\sigma_{e_{SD}}^2\rho_s + 1}\right.\\ &\qquad \left. + \frac{g_{RD}b_1\rho_r}{g_{RD}b_2\rho_r + \kappa\sigma_{e_{RD}}^2\rho_r + 1} > x\right\}\end{aligned} \tag{12}$$

It is difficult to derive the exact expression of the CCDF of the user1 SINR directly, so an approximate analysis of the CCDF of the UE1's SINR was derived. Also, letting $\hat{\lambda}_{SR} \triangleq \left|\hat{h}_{SR}\right|^2$, $\hat{\lambda}_{RD} \triangleq \left|\hat{h}_{RD}\right|^2$, $\hat{\lambda}_{SD} \triangleq \left|\hat{h}_{SD}\right|^2$, using [18] the probability density function (PDF) $f_{\left|h_\phi\right|^2}(x) = (1/\beta_\phi)e^{-x/\beta_\phi}$, where $\phi \in \{SR, SD, RD\}$. The approximate expression for the CCDF of the SINR for UE1 is given as:

$$\begin{aligned}&\overline{F}_{SINR_1}(x)\\ &= \Pr\left(\min(\gamma_R^1, \gamma_D^1) > x\right)\\ &\approx \Pr\left\{\frac{g_{SR}a_1\rho_s}{g_{SR}a_2\rho_s + \kappa\sigma_{e_{SR}}^2\rho_s + 1} > x, \frac{g_{SD}a_1\rho_s}{g_{SD}a_2\rho_s + \kappa\sigma_{e_{SD}}^2\rho_s + 1} + \frac{b_1}{b_2} > x\right\}\\ &= \Pr\left\{\hat{\lambda}_{SR} > \frac{\chi_{SR}xD_1}{(a_1 - xa_2)\rho_S}\right\} \cdot \Pr\left\{\lambda_{SD} > \frac{\chi_{SD}\tau D_3}{(a_1 - \tau a_2)\rho_S}\right\}\\ &= \int_{\chi_{SR}\psi(x)}^{0} \frac{1}{\beta_{SR}} e^{-\frac{u}{\beta_{SR}}} du \cdot \int_{\chi_{SD}\psi(\tau)}^{0} \frac{1}{\beta_{SD}} e^{-\frac{v}{\beta_{SD}}} dv\\ &= e^{-\left(\frac{\chi_{SR}\psi(x)}{\beta_{SR}} + \frac{\chi_{SD}\psi(\tau)}{\beta_{SD}}\right)}\end{aligned} \tag{13}$$

Where $a_1 > xa_2$, $\rho_s = P_S/\sigma^2$, $\rho_r = P_R/\sigma^2$. The above process completes the proof of the CDF of the SINR for UE1.

Proof complete.

Theorem 2: The CDF of the SINR for UE2 is given as:

$$F_{SINR_2}(x) = 1 - \xi_1 e^{-(\omega_1 + \omega_2)x} + \xi_2 e^{-(\omega_1 + \omega_3)x} \tag{14}$$

Where $\omega_1 = \frac{\chi_{SR}D_1}{a_2\rho_s\beta_{SR}}$, $\omega_2 = \frac{\chi_{SD}D_3}{a_2\rho_s\beta_{SD}}$, $\omega_3 = \frac{\chi_{RD}D_2}{b_2\rho_r\beta_{RD}}$, $\xi_1 = \frac{a_2\chi_{RD}\rho_s\beta_{SD}/D_3}{a_2\chi_{RD}\rho_s\beta_{SD}/D_3 - b_2\chi_{SD}\rho_r\beta_{RD}/D_2}$, $\xi_2 = \frac{b_2\chi_{SD}\rho_r\beta_{RD}/D_2}{a_2\chi_{RD}\rho_s\beta_{SD}/D_3 - b_2\chi_{SD}\rho_r\beta_{RD}/D_2}$.

Proof: The CDF of the SINR for UE2 is proved as follows.

Similarly, the derived expression for the CCDF of the SINR for UE2 is as follows:

$$
\begin{aligned}
&\overline{F}_{SINR_2}(x) \\
&= \Pr\left(\min(\gamma_R^2, \gamma_D^2) > x\right) \\
&= \Pr\left\{\frac{g_{SR}a_2\rho_s}{\kappa\sigma_{e_{SR}}^2\rho_s+1} > x, \frac{g_{SD}a_2\rho_s}{\kappa\sigma_{e_{SR}}^2\rho_s+1} + \frac{g_{RD}b_2\rho_r}{\kappa\sigma_{e_{RD}}^2\rho_r+1} > x\right\} \\
&= \Pr\left\{\hat{\lambda}_{SR} > \frac{\chi_{SR}xD_1}{a_2\rho_S}\right\} \cdot \Pr\left\{\frac{g_{SD}a_2\rho_s}{\kappa\sigma_{e_{SR}}^2\rho_s+1} + \frac{g_{RD}b_2\rho_r}{\kappa\sigma_{e_{RD}}^2\rho_r+1} > x\right\} \\
&= e^{-\frac{\chi_{SR}xD_1}{a_2\rho_s\beta_{SR}}} \cdot \left\{1 - \int_0^{\frac{\chi_{SD}xD_3}{a_2\rho_s}} \int_0^{\frac{(x-\frac{ua_2\rho_s}{\chi_{SD}D_3})\chi_{RD}D_2}{b_2\rho_r}} \frac{1}{\beta_{RD}} e^{-\frac{v}{\beta_{RD}}} dv \cdot \frac{1}{\beta_{SD}} e^{-\frac{u}{\beta_{SR}}} du\right\} \\
&= \xi_1 e^{-(\omega_1+\omega_2)x} - \xi_2 e^{-(\omega_1+\omega_3)x}
\end{aligned}
\tag{15}
$$

Proof completed.

3.1 Average Achievable Rate

According to (8) and (10), the average achievable rate of UE1 in the UAV cooperative NOMA communication system can be derived as follows:

$$
\begin{aligned}
C_{x_1} &= \int_0^{\infty} \frac{1}{2}\log_2(1+x) f_{SINR_1}(x)dx \\
&= \frac{1}{2\ln 2}\int_0^{\frac{a_1}{a_2}} \frac{1-F_{SINR_1}(x)}{1+x}dx \\
&= \frac{1}{2\ln 2}\int_0^{\frac{a_1}{a_2}} \frac{1}{1+x} e^{-\left(\frac{\chi_{SR}\psi(x)}{\beta_{SR}} + \frac{\chi_{SD}\psi(\tau)}{\beta_{SD}}\right)}dx
\end{aligned}
\tag{16}
$$

Similarly, based on (9) and (14), the average achievable rate of UE2 signal is obtained as follows:

$$
\begin{aligned}
C_{x_2} &= \int_0^{\infty} \frac{1}{2}\log_2(1+x) f_{SINR_2}(x)dx \\
&= \frac{1}{2\ln 2}\int_0^{\infty} \frac{1-F_{SINR_2}(x)}{1+x}dx \\
&= \frac{1}{2\ln 2}\int_0^{\infty} \frac{1}{1+x}\left(\xi_1 e^{-(\omega_1+\omega_2)x} + \xi_2 e^{-(\omega_1+\omega_3)x}\right)dx \\
&= -\frac{\xi_1}{2\ln 2} e^{\omega_1+\omega_2} Ei\left(-\omega_1-\omega_2\right) \\
&\quad + \frac{\xi_2}{2\ln 2} e^{\omega_1+\omega_3} Ei\left(-\omega_1-\omega_3\right)
\end{aligned}
\tag{17}
$$

Where $\int_0^{\infty} \frac{e^{-mx}}{1+x}dx = -e^m Ei(-m)$, $Ei(\cdot)$ is an exponential integral function.

Combining (16) and (17), the average achievable rate of the cooperative NOMA system is given as:

$$\begin{aligned} C_{NOMA} &= C_{x_1} + C_{x_2} \\ &= \frac{1}{2\ln 2}\int_0^{\frac{a_1}{a_2}} \frac{1}{1+x} e^{-\left(\frac{\chi_{SR}\psi(x)}{\beta_{SR}} + \frac{\chi_{SD}\psi(\tau)}{\beta_{SD}}\right)} dx \\ &\quad - \frac{\xi_1}{2\ln 2} e^{\omega_1+\omega_2} Ei\left(-\omega_1-\omega_2\right) \\ &\quad + \frac{\xi_2}{2\ln 2} e^{\omega_1+\omega_3} Ei\left(-\omega_1-\omega_3\right) \end{aligned} \tag{18}$$

3.2 Outage Probability Analysis

If the transmission rate of the signal in the communication system is less than the threshold rate, the communication will be failed. Therefore, the outage probability is also an important indicator of the wireless communication system. Let R_1, R_2 be the target rate for UE1 and UE2. According to Shannon's theorem, the outage events of UE1 occur when $C_{x_1} < R_1$. The outage probability for UE1 is given as:

$$\begin{aligned} P_{x_1} &= \Pr\left\{C_{x_1} < R_1\right\} = \Pr\left\{\frac{1}{2}\log_2(1+\min(\gamma_R^1, \gamma_D^1)) < R_1\right\} \\ &= \Pr\left\{SINR_1 < 2^{2R_1} - 1\right\} = \Pr\left\{SINR_1 < \phi_1\right\} \\ &= 1 - \Pr\left\{SINR_1 > \phi_1\right\} = 1 - \Pr\left\{\gamma_R^1 > \phi_1, \gamma_D^1 > \phi_1\right\} \end{aligned} \tag{19}$$

Where $\phi_1 = 2^{2R_1} - 1$.

The probability of successful communication for UE1 is given as:

$$\begin{aligned} \overline{P}_{x_1} &= \Pr\left\{\gamma_R^1 > \phi_1, \gamma_D^1 > \phi_1\right\} \\ &= \Pr\left\{\frac{g_{SR}a_1\rho_s}{g_{SR}a_2\rho_s + \kappa\sigma_{e_{SR}}^2\rho_s + 1} > \phi_1,\right. \\ &\qquad \left.\frac{g_{SD}a_1\rho_s}{g_{SD}a_2\rho_s + \kappa\sigma_{e_{SD}}^2\rho_s + 1} + \frac{b_1}{b_2} > \phi_1\right\} \\ &= \Pr\left\{\hat{\lambda}_{SR} > \frac{\chi_{SR}\phi_1}{(a_1 - \phi_1 a_2)\rho_S}\right\} \cdot \Pr\left\{\lambda_{SD} > \frac{\chi_{SD}\theta}{(a_1 - \theta a_2)\rho_S}\right\} \\ &= e^{-\left(\frac{\chi_{SR}\psi(\phi_1)}{\beta_{SR}} + \frac{\chi_{SD}\psi(\theta)}{\beta_{SD}}\right)} \end{aligned} \tag{20}$$

The outage probability for UE1 is given as:

$$P_{x_1} = 1 - e^{-\left(\frac{\chi_{SR}\psi(\phi_1)}{\beta_{SR}} + \frac{\chi_{SD}\psi(\theta)}{\beta_{SD}}\right)} \tag{21}$$

Similarly, the outage events of UE2 occur when $C_{x_2} < R_2$. The outage probability for UE2 is given as:

$$\begin{aligned} P_{x_2} &= \Pr\left\{C_{x_2} < R_2\right\} = \Pr\left\{\frac{1}{2}\log_2(1+\min(\gamma_R^2, \gamma_D^2)) < R_2\right\} \\ &= \Pr\left\{SINR_2 < 2^{2R_2} - 1\right\} = \Pr\left\{SINR_2 < \phi_2\right\} \\ &= 1 - \Pr\left\{SINR_2 > \phi_2\right\} = 1 - \Pr\left\{\gamma_R^2 > \phi_2, \gamma_D^2 > \phi_2\right\} \end{aligned} \tag{22}$$

Where $\phi_2 = 2^{2R_2} - 1$.

The probability of successful communication for UE2 is given as:

$$\begin{aligned}\overline{P}_{x_2} &= \Pr\left\{\gamma_R^2 > \phi_2, \gamma_D^2 > \phi_2\right\} \\ &= \Pr\left\{\frac{g_{SR}a_2\rho_s}{\kappa\sigma_{e_{SR}}^2\rho_s+1} > x, \frac{g_{SD}a_2\rho_s}{\kappa\sigma_{e_{SD}}^2\rho_s+1} + \frac{g_{SD}b_2\rho_r}{\kappa\sigma_{e_{RD}}^2\rho_r+1} > x\right\} \\ &= \Pr\left\{\hat{\lambda}_{SR} > \frac{\chi_{SR}x}{a_2\rho_S}\right\} \cdot \Pr\left\{\frac{g_{SD}a_2\rho_s}{\kappa\sigma_{e_{SD}}^2\rho_s+1} + \frac{g_{SD}b_2\rho_r}{\kappa\sigma_{e_{RD}}^2\rho_r+1} > x\right\} \\ &= \xi_1 e^{-(\omega_1+\omega_2)\phi_2} - \xi_2 e^{-(\omega_1+\omega_3)\phi_2}\end{aligned} \tag{23}$$

The outage probability for UE2 is given as:

$$P_{x_2} = 1 - \xi_1 e^{-(\omega_1+\omega_2)\phi_2} + \xi_2 e^{-(\omega_1+\omega_3)\phi_2} \tag{24}$$

Based on the outage probability of UE1 and UE2, the total outage probability of the communication system can be expressed as follows:

$$\begin{aligned}P_{NOMA} &= 1 - \overline{P}_{x_1} \cdot \overline{P}_{x_2} \\ &= 1 - e^{-\left(\frac{\chi_{SR}\psi(\phi_1)}{\beta_{SR}} + \frac{\chi_{SD}\psi(\theta)}{\beta_{SD}}\right)} \cdot (\xi_1 e^{-(\omega_1+\omega_2)\phi_2} - \xi_2 e^{-(\omega_1+\omega_3)\phi_2})\end{aligned} \tag{25}$$

3.3 Throughput

Throughput is the amount of data that the system successfully transmits signals, that is, the average amount of information successfully transmitted per communication. Throughput, like average achievable rate and outage probability, is also a crucial metric for evaluating the communication performance of the system.

$$\begin{aligned}R_{NOMA} &= (R_1 + R_2)(1 - P_{NOMA}) \\ &= (R_1 + R_2)e^{-\left(\frac{\chi_{SR}\psi(\phi_1)}{\beta_{SR}} + \frac{\chi_{SD}\psi(\theta)}{\beta_{SD}}\right)} \cdot (\xi_1 e^{-(\omega_1+\omega_2)\phi_2} - \xi_2 e^{-(\omega_1+\omega_3)\phi_2})\end{aligned} \tag{26}$$

In the above equation, $1 - P_{NOMA}$ denotes the probability of that system will successfully transmit the signal.

4 Simulation Results

In this section, to verify the correctness of the theoretical derivations, Monte Carlo simulations were conducted for the UAV relay communication system under Rayleigh fading channels. The average achievable rate, outage probability, and throughput of the system were analyzed through MATLAB computer simulations. In the simulation, the distance between the source and the destination is denoted as c = 100 m. The horizontal distance from the source to the relay is denoted as d_1 = 42 m. The channel estimation error variance is denoted as $\sigma_{e_i}^2 = 1$. The channel parameters are set as follows: In the first scenario, $\beta_{SR} = \beta_{RD} = 10$, $\beta_{SD} = 5$, and in the second scenario, $\beta_{SR} = 6$, $\beta_{RD} = 10$, $\beta_{SD} = 5$. The power allocation factors for the source and relay are set as $a_1 = 0.9$, $a_2 = 0.1$.

Fig. 2 illustrates the curve of average achievable rate versus SNR of the source. It compares the proposed NOMA system with the cooperative NOMA system from [19], UAV altitude is set to H=120m and the transmit SNR of the relay is $\rho_r = 10dB$, the path loss coefficient is set to $\alpha_T = 0.5$. The Monte Carlo simulation results match the theoretical expressions perfectly, which confirms the accuracy of the theoretical derivations. As shown in the graph, the achievable rate of the system significantly increases with the rise of SNR. Regardless of the specific value of the SNR of the source, the average achievable rate of the proposed NOMA system is analyses better

than the average achievable rate of NOMA system in [19]. With the increase in the SNR, the average achievable rate of the NOMA system in [19] reaches a constant value. This is due to the fact that in the source-to-destination pass-through link, UE2 signal is not decoded and utilized at the destination end, and the SNR of UE2 signal is limited by a fixed value of ρ_r.

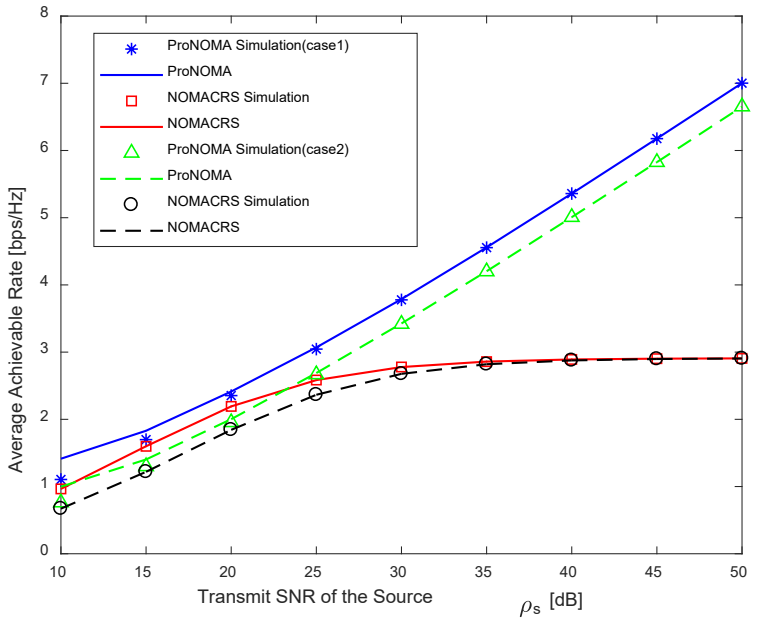

Fig. 2. Comparative plot of average reachable rate versus the transmit SNR of the source ρ_s

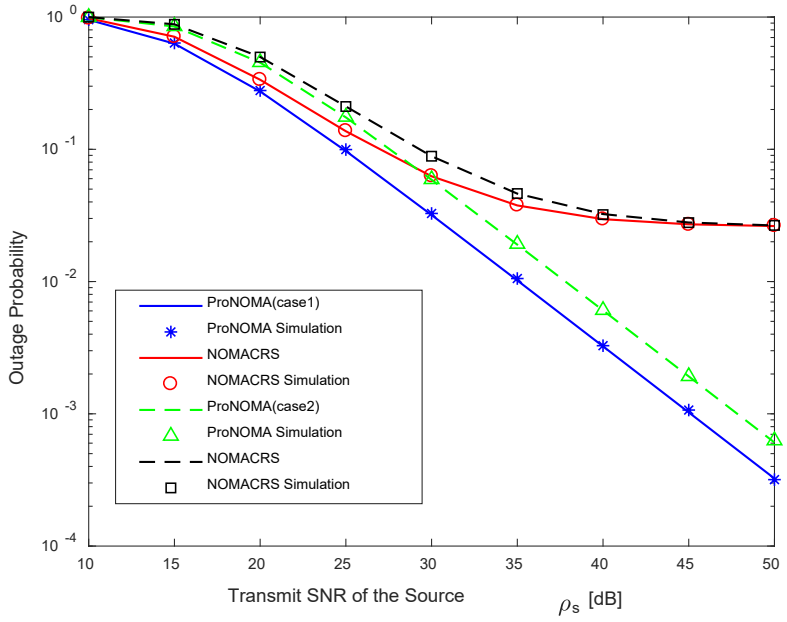

Fig. 3. Comparison of Outage Probability versus the transmit SNR of the source ρ_s

Fig. 3 shows the variation of the system outage probability with the SNR of the source. In this case, the altitude is set to H=120m, the transmit SNR of the relay is $\rho_r = 10dB$, $\alpha_T = 0.5$, and the target rate is $R_1 = R_2 = 1$(bps/*Hz*). From the graph, it can be observed that as the SNR increases, the system's outage probability gradually decreases. At the higher SNR, the outage performance of the proposed scheme outperforms the outage performance of the NOMA scheme in [19].

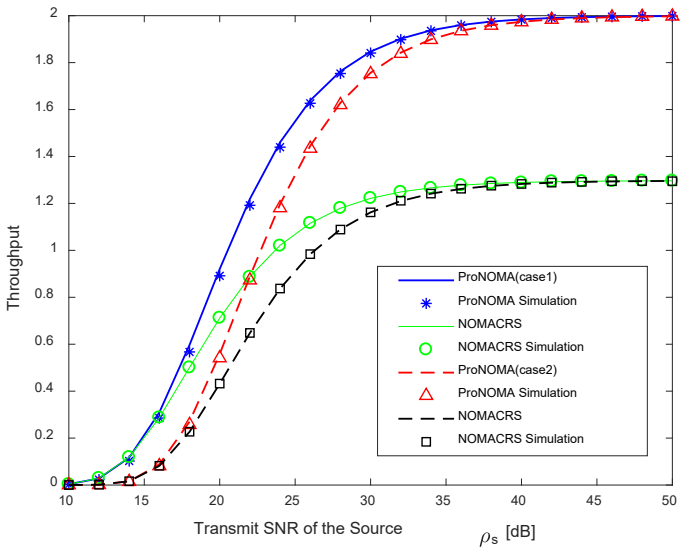

Fig. 4. Comparison of System Throughput versus the transmit SNR of the source ρ_s

Fig. 4 analyzes the curve of system throughput with respect to the SNR of the source, setting the target rate thresholds for UE1 and UE2 as $R_1 = R_2 = 1$(bps/*Hz*). The SNR of the relay is set to $\rho_r = 10dB$, and the path loss coefficient is set to $\alpha_T = 0.5$. From the graph, the figure shows that at high SNR, the throughput performance of the proposed scheme outperforms the system performance in NOMA [19]. In additional, under high SNR, the throughput of both systems gradually approaches an upper limit. The value of this upper limit is the sum of the target transmission rates for UE1 and UE2. This is due to the fact that at high transmission SNR, the outage probability of the system is nearly zero, and the probability of successful transmission approaches 1. Therefore, the probability of a successful system has little effect on system throughput. Thus, with a high SNR of the source, the throughput of the systems is primarily influenced by the target transmission rates.

Fig. 5 and Fig. 6 illustrate the impact of channel estimation errors on system performance. The target rate thresholds for UE1 and UE2 are $R_1 = R_2 = 1$(bps/*Hz*). The SNR of the relay is $\rho_r = 10dB$, and the path loss coefficient is $\alpha_T = 0.5$. Under channel conditions for the first scenario $\beta_{SR} = \beta_{RD} = 10$, $\beta_{SD} = 5$, the graphs depict the variation of system average achievable rates with respect to SNR for different estimation error coefficients. It can be observed from the graphs that a larger error factor leads to the poorer system average achievable rate performance. A bigger κ indicates a severer imperfect impact. Accurate channel estimation is particularly crucial for system improvement. Fig. 6 illustrates the impact of different estimation error factors on the system's outage probability performance with different SNR. It can be seen from the graph that a larger estimation error factor results in poorer outage probability performance for the system.

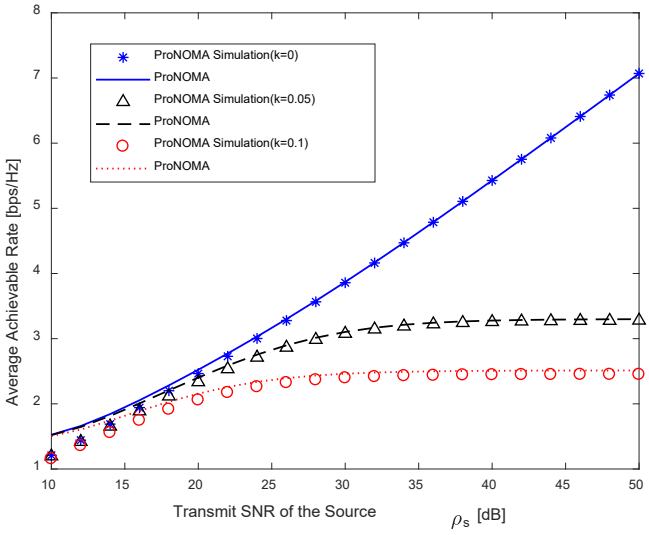

Fig. 5. Comparison of average achievable rates versus the transmit SNR of the source ρ_s under different estimation error factors

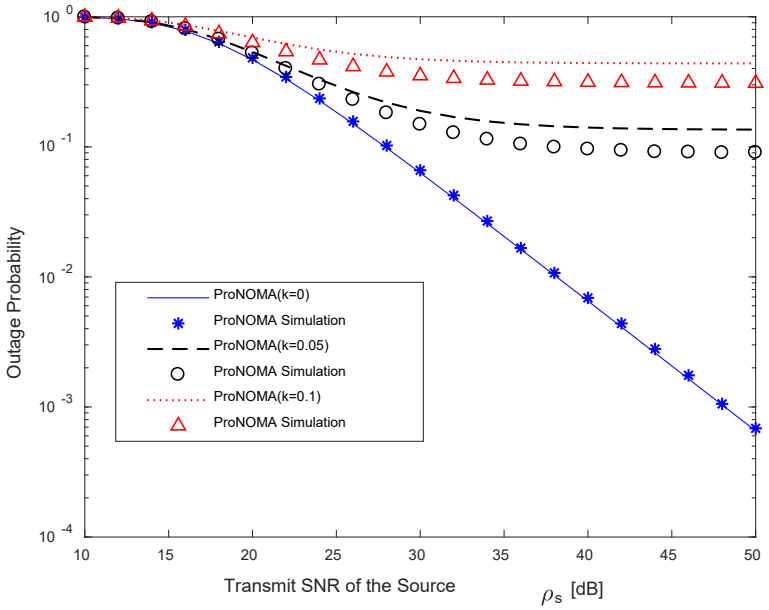

Fig. 6. Comparison of outage probability versus the transmit SNR of the source ρ_s under different estimation error factors

To verify the impact of path loss coefficients on system performance, the relationship between outage probability and the SNR of the source is compared with under different link loss coefficients in Fig. 7. We assumed the channel conditions belong to first scenario, where H=120m, and the SNR of the relay is set to $\rho_r = 20dB$. The system's target transmission rate is set to $R_1 = R_2 = 1$(bps/Hz). As observed from the graph, the outage probability performance gradually deteriorates with the increase of link loss coefficients. This is due to the fact that the larger the link loss coefficients, the smaller the channel gain. Moreover, under the same SNR of the source conditions, an increase in path loss coefficients leads to a higher outage probability.

Fig. 8 illustrates the system's throughput versus the SNR under different link loss coefficients. It can be observed that a larger path loss coefficient corresponds to poorer throughput performance. However, eventually converge to an upper limit, which is the sum of the target transmission rate thresholds for UE1 and UE2. This upper limit is mainly influenced by the target rate.

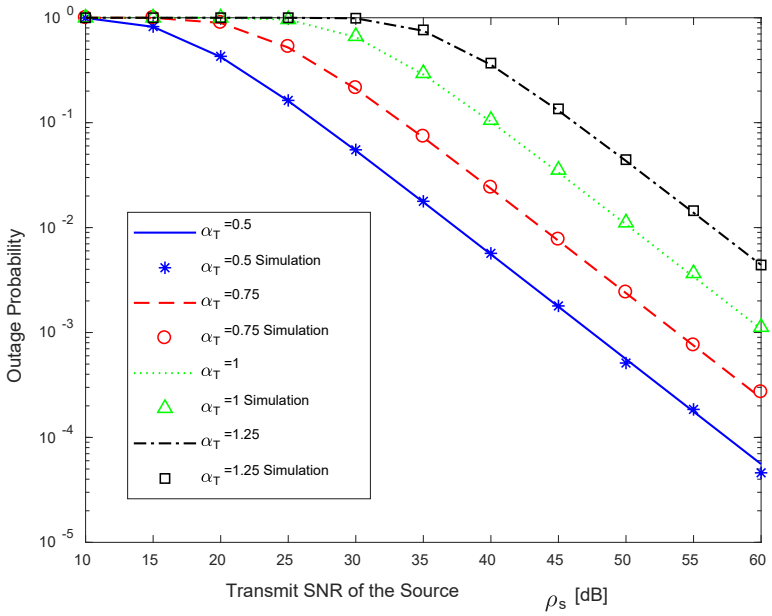

Fig. 7. Comparison graph of outage probability versus the transmit SNR of the source ρ_s under different link loss coefficients

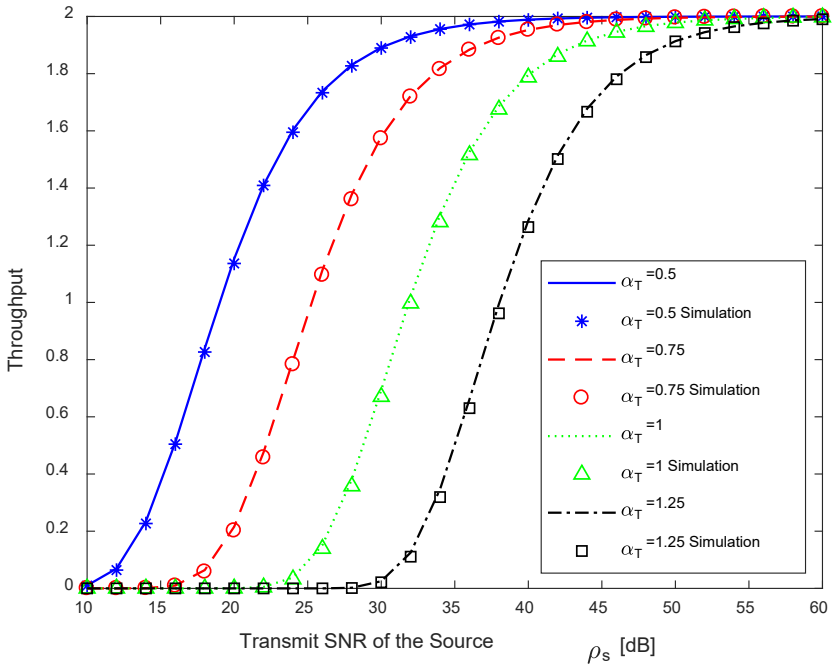

Fig. 8. Comparison of system throughput versus the transmit SNR of the source ρ_s under different path loss coefficients

Fig. 9 illustrates the variation of the average achievable rate with the SNR of the source under different SNR of the relay. Under ideal conditions, with a UAV altitude of H=120m and the channel conditions corresponding to the first case, the higher the relay transmission SNR, the better the system average achievable rate performance. For a fixed SNR of the source, the average achievable rate increases with the SNR of the relay.

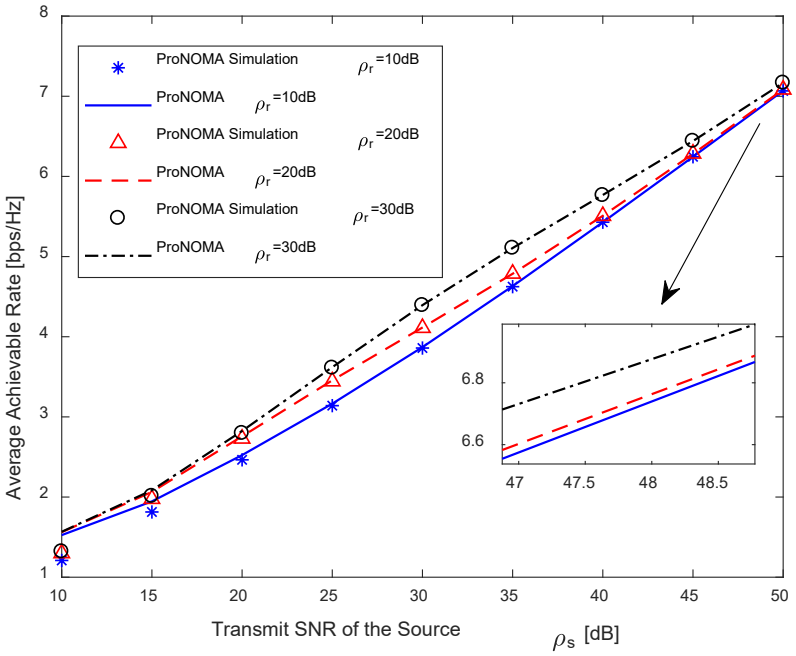

Fig. 9. Comparison of system throughput versus the transmit SNR of the source ρ_s under different path loss coefficients

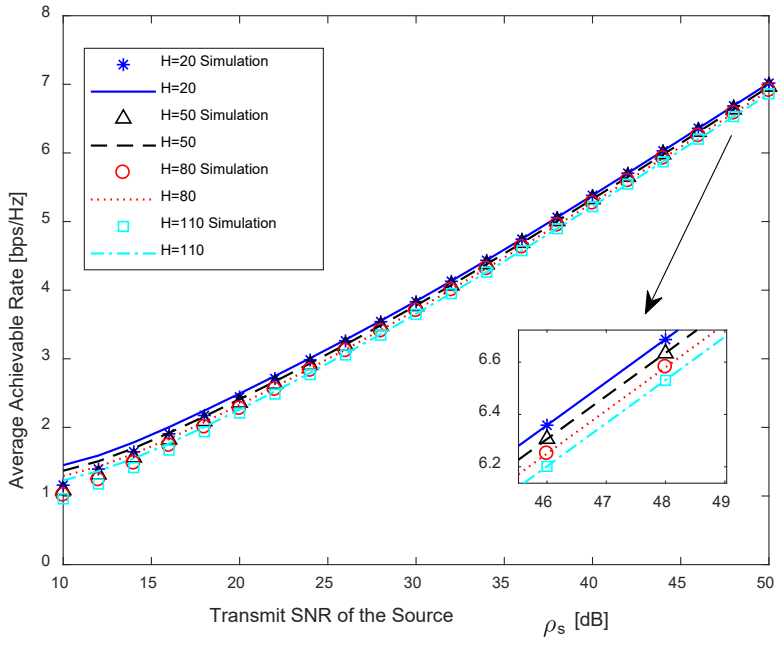

Fig. 10. Comparison of system throughput versus the transmit SNR of the source ρ_s under different path loss coefficients

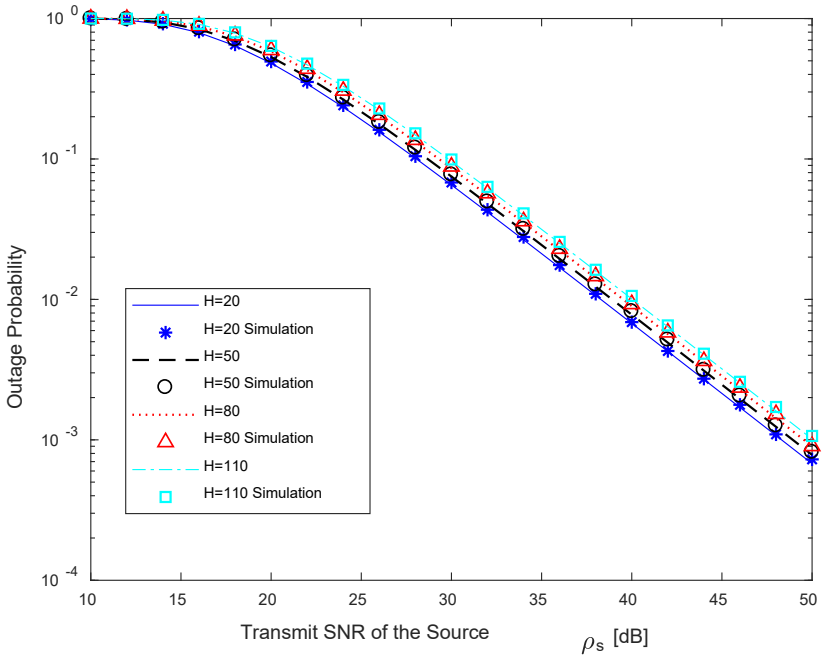

Fig. 11. Comparison of system throughput versus the transmit SNR of the source ρ_s under different path loss coefficients

Fig. 10 illustrates the curve of the system's average achievable rate as the SNR of the source changes with different UAV flying altitudes. Fig. 11 illustrates a comparison of the system's outage probability under varying SNR of the source for different UAV flying altitudes. Setting $R_1 = R_2 = 1$(bps/Hz), ρ_r =10dB, $\alpha_T = 0.5$, under the second channel condition. It can be observed from the figures that the performance of the average achievable rate and outage probability of the system gradually decrease with the increase of altitude. This is because as the horizontal distance d_1 increases, the link channel gain decreases, which lead to decline in both the average achievable rate and outage probability performance of the entire system. Under a constant SNR of the source, the higher the altitude of the UAV, the lower the performance of the average achievable rate, and the higher the performance of the outage probability.

5 Conclusion

This paper investigates the communication performance of UAV cooperative NOMA system and compares it with the NOMA system in [19]. The expressions for the system's average achievable rate, outage probability, and throughput are theoretically derived. The accuracy of these theoretical expressions is confirmed through Monte Carlo simulations. The numerical results indicated that the UAV cooperative NOMA system achieved a remarkable gain over the NOMA system in [19]. The results will help to combine cooperative jamming with the UAV cooperative NOMA system to achieve better system security performance in future research.

6 Acknowledgment

This research was supported by the National Natural Science Foundation of China under grant 61841107 and 62061024, Gansu natural science foundation under grant 22JR5RA274 and 23YFGA0062, Gansu Innovation Foundation 2022A-215.

References

[1] M. Mozaffari, W. Saad, M. Bennis, Y.-H. Nam, M. Debbah, A Tutorial on UAVs for Wireless Networks: Applications, Challenges, and Open Problems, IEEE Communications Surveys & Tutorials 21(3)(2019) 2334-2360. https://doi.org/10.1109/COMST.2019.2902862

[2] N.H. Motlagh, T. Taleb, O. Arouk, Low-Altitude Unmanned Aerial Vehicles-Based Internet of Things Services: Comprehensive Survey and Future Perspectives, IEEE Internet of Things Journal 3(6)(2016) 899-922. https://doi.org/10.1109/JIOT.2016.2612119

[3] Y.L. Liu, H.N. Dai, Q.B.J. Wang, Unmanned aerial vehicle enabled communication technologies and applications for Internet of things, Chinese Journal on Internet of Things 3(4)(2019) 48-55. https://doi.org/10.11959/j.issn.2096-3750.2019.00131

[4] D. Yang, Q. Wu, Y. Zeng, R. Zhang, Energy Tradeoff in Ground-to-UAV Communication via Trajectory Design, IEEE Transactions on Vehicular Technology 67(7)(2018) 6721-6726. https://doi.org/10.1109/TVT.2018.2816244

[5] J. Yang, J. Chen, Z. Yang, Energy-Efficient UAV Communication With Trajectory Optimization, in: Proc. 2021 2nd International Conference on Big Data & Artificial Intelligence & Software Engineering (ICBASE), 2021. https://doi.org/10.1109/ICBASE53849.2021.00100

[6] H. Ghazzai, M.B. Ghorbel, A. Kadri, M.J. Hossain, H. Menouar, Energy-Efficient Management of Unmanned Aerial Vehicles for Underlay Cognitive Radio Systems, IEEE Transactions on Green Communications and Networking 1(4)(2017) 434-443. https://doi.org/10.1109/TGCN.2017.2750721

[7] X. Qin, Z. Song, Y. Hao, X. Sun, Joint Resource Allocation and Trajectory Optimization for Multi-UAV-Assisted Multi-Access Mobile Edge Computing, IEEE Wireless Communications Letters 10(7)(2021) 1400-1404. https://doi.org/10.1109/LWC.2021.3068793

[8] B.P. Chaudhary, R.K. Mishra, Performance Analysis of SWIPT Cooperative-NOMA Over Rayleigh Fading Channel, in: Proc. 2023 15th International Conference on Computer and Automation Engineering (ICCAE), 2023. https://doi.org/10.1109/ICCAE56788.2023.10111338

[9] Y. Li, Y.Z. Li, X.L. Chu, Y.H. Ye, H.L. Zhang, Performance Analysis of Relay Selection in Cooperative NOMA Networks, IEEE Communications Letters 23(4)(2019) 760-763. https://doi.org/10.1109/LCOMM.2019.2898409

[10] Y.H. Feng, Z. Yang, W.-P. Zhu, Q. Li, B. Lv, Robust Cooperative Secure Beamforming for Simultaneous Wireless Information and Power Transfer in Amplify-and-Forward Relay Networks, IEEE Transactions on Vehicular Technology 66(3)(2017) 2354-2366. https://doi.org/10.1109/TVT.2016.2578313

[11] N. Sachdeva, V.B. Kumaravelu, P. Selvaprabhu, H. Sheeba J, C.S. Evangeline, A.L. Imoize, Probability of Error Analysis of Decode-and-Forward Cooperative Relaying System with Maximal Ratio Combining, in: Proc. 2023 2nd International Conference on Vision Towards Emerging Trends in Communication and Networking Technologies (ViTECoN), 2023. https://doi.org/10.1109/ViTECoN58111.2023.10157570

[12] P.K. Sharma, D.I. Kim, UAV-Enabled Downlink Wireless System with Non-Orthogonal Multiple Access, in: Proc. 2017 IEEE Global Communications Conference (GC Wkshps), 2017. https://doi.org/10.1109/GLOCOMW.2017.8269066

[13] Y. Liu, Z. Qin, Y. Cai, G. Li, A. Nallanathan, UAV Communications Based on Non-Orthogonal Multiple Access, IEEE Wireless Communications 26(1)(2019) 52-57. https://doi.org/10.1109/MWC.2018.1800196

[14] X.L. Sun, W.W. Yang, Y.M. Cai, Secure communication in NOMA-assisted millimeter-wave SWIPT UAV networks, IEEE Internet of Things Journal 7(3)(2020) 1884-1897. https://doi.org/10.1109/JIOT.2019.2957021

[15] X. Li, Q. Wang, H. Peng, H. Zhang, D.T. Do, K.M. Rabie, R. Kheral, C.C. Cavalcante, A unified framework for HS-UAV NOMA networks: Performance analysis and location optimization, IEEE Access 8(2020) 13329-13340. https://doi.org/10.1109/ACCESS.2020.2964730

[16] X. Liu, J. Wang, N. Zhao, Y. Chen, S. Zhang, Z. Ding, F.R. Yu, Placement and power allocation for NOMA-UAV networks, IEEE Wireless Communications Letters 8(3)(2019) 965-968. https://doi.org/10.1109/LWC.2019.2904034

[17] M.R. Bhatnagar, On the capacity of decode-and-forward relaying over Rician fading channels, IEEE Communications Letters 17(6)(2013) 1100-1103. https://doi.org/10.1109/LCOMM.2013.050313.122813

[18] Y.Y. Cai, J.Y. Bao, L.C. Chen, Probability Theory and Mathematical Statistics, Economic Science Press, Beijing, 2022.

[19] J.-B. Kim, I.-H. Lee, Capacity Analysis of Cooperative Relaying Systems Using Non-Orthogonal Multiple Access, IEEE Communications Letters 19(11)(2015) 1949-1952. https://doi.org/10.1109/LCOMM.2015.2472414